Experimental Study on Wetting of Fibers with Non-Newtonian Liquids

Mamdouh T. Ghannam and M. Nabil Esmail
Dept. of Chemical Engineering, University of Saskatchewan, Saskatoon, Canada S7N 5C9

Parameters of wetting dry fibers with non-Newtonian liquids are studied experimentally. Rheological tests show that seven of the 13 test liquids adhere to Newtonian behavior with a wide range of viscosities $3 < \mu < 30{,}000$ mPa·s. The other six liquids show shear-thinning behavior with different flow indices. Some of the liquids exhibited viscoelastic behavior. Diameters of the fibers are in the range $0.033 < D < 0.071$ cm. Experimental measurements cover contact angles, interfacial depths and diameters, as well as the critical wetting speed of entraining visible small air bubbles in the liquid volume. Dynamic contact angles are strong functions of the apparent viscosity of the liquid at the particular wetting speed regardless of whether the liquid is Newtonian or non-Newtonian. Higher values of contact angles correspond to wetting of fiber with larger diameter for less viscous liquids. Critical capillary numbers of air entrainment for shear thinning liquids are generally higher than those for Newtonian liquids. Depressions created in the surface of different test liquids can be classified into three different scales, corresponding to three scales of liquid viscosities.

Introduction

The dynamics of wetting of solid surfaces with a layer of liquid is an important area of research because of the multitude of fundamental fluid and surface phenomena that it continues to reveal. It is also an area of many industrial applications. Many emerging technologies include a coating process where a solid surface of a certain shape has to be covered by a layer of liquid coating. Examples of such processes are in the production of photo-materials, electronic storage devices, various tapes, print paper, and fiber-optic cables. The mechanics of liquid coating are greatly influenced by the combined abilities of the liquid and solid to achieve complete wetting at the given speeds of solid motion. Industrial coating processes usually require complete coverage of the solid surface by a liquid layer of a certain uniform thickness. Conditions that lead to complete wetting depend on the properties of liquid and solid, and the dynamic parameters of the process. The focus of the coating process is on the so-called contact line, where the liquid replaces air on the solid surface as coverage. The theory of fluid mechanics is not structured to deal with solid-liquid interfaces other than those where the liquid experiences either complete adherence to the solid (no-slip), or complete slippage over the surface. The contact line of a wetting process does not comply with either of these limiting cases. In the absence of rigorous theoretical analysis of wetting at the contact line, experimental studies are extremely important. In fact, experimental measurements of the conditions at the contact line are often used as input data in theoretical computations of the fluid dynamics in that region.

Dynamic contact angles are the angles formed between the liquid meniscus and the wet substrate close to the contact line. At static conditions, static contact angles are known to depend on the balance of surface energies and gravity at the line. In a coating process, the solid surface is steadily moving and the contact angle departs from its static value nonlinearly increasing within the range of complete wetting. At higher substrate speeds, the contact line loses its dynamic stability and visible air bubbles may be entrained into the coating layer.

Dynamic contact lines and air entrainment are important factors in fiber coating. Fibers are usually drawn through a cup filled with the coating liquid. Until recent years, silicone was frequently used in fiber-optics production as a coating liquid. Many polymer solutions have now replaced silicone in providing a protective coating layer. Double-layer coating of fibers is now common in recent technology.

There is a large volume of work in literature on wetting studies. Some of these studies focused on dynamic contact

angles and air entrainment (Gutoff and Kendrick, 1982; Joos et al., 1990; Ghannam and Esmail, 1990; Burley, 1992; Miyamoto, 1991; Perry, 1967). For a detailed account of previous work, one may consult Blake (1988) and Ghannam (1991). In previous work Ghannam and Esmail (1993) studied the wetting of fibers using glycerol solutions as test liquids. Glycerol solutions are Newtonian over the entire wide range of viscosities that they provide $1 < \mu < 1{,}000$ mPa·s. This study reports our experimental measurements of the basic parameters of the dynamics of wetting of fibers with non-Newtonian liquids. The purpose is to investigate the differences between these parameters and their counterparts in the case of Newtonian liquids, and to generate some inventory of experimental measurements of wetting parameters with non-Newtonian liquids.

Experimental Studies

A Plexiglas tank with dimensions $25 \times 15 \times 10$ cm served as a liquid bath (Figure 1). Plastic monofilament fibers ran over a system of guide, tension, and drive pulleys to vertically enter the liquid bath. The point of entry was at least 7 cm away from the bath walls. Fibers of four different diameters were used during the tests. The diameters are listed in Table 1. All experiments were conducted with the fiber line of the diameter 0.033 cm, except those dealing with comparisons between different fiber diameters. The fibers had sufficiently high tensile strength for the tension experienced by the line.

A variable speed motor provided the driving force to the system at different speeds. This motor could pull the fiber line with steady linear speeds higher than $V = 2$ cm/s. The fiber constant speed was measured in rpm by a high precision Computak Tachometer.

Liquids

Thirteen test liquids were investigated in the study, which were chosen to cover a rather wide range of rheological behavior. Table 2 shows the physical and rheological properties of the test liquids. ($\dot{\gamma}$ is the shear rate (s^{-1}), and τ is shear stress (Pa).) Glycerol analytical reagent from BDH Inc. was used in full and 95% concentrations (Gly100, and Gly95). Poly(dimethylsiloxane) 200 fluid from Aldrich Chemical

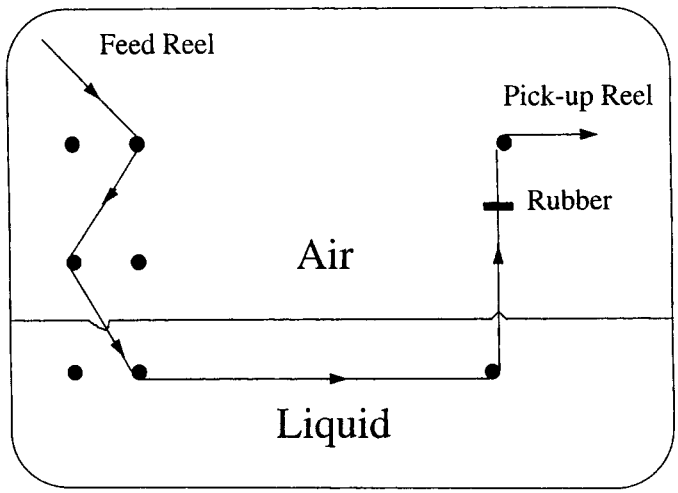

Figure 1. Experimental setup.

Table 1. Fiber Diameters

Fiber Line Specification	Dia., cm
10 lb (4.5 kg) test/force	0.0330
20 lb (9.1 kg) test/force	0.0483
30 lb (13.6 kg) test/force	0.0584
40 lb (18.2 kg) test/force	0.0711

Company Inc. was used in two different viscosities 1,000 (PDMS1) and 25,000 (PDMS30) mPa·s. Polydimethylsiloxane is a silicon polymer developed for use as a dielectric coolant and in solar energy installations. It is highly resistant to oxidation and to biodegradation by microorganisms. Silicone rubber systems based on polydimethylsiloxane are examples of thermal cure systems that have low glass transition temperature (-50 to -125°C) and low modulus of elasticity (10^6 to 10^7 dyne/cm^2). This makes these organic materials extremely effective buffer coatings, and they are commonly used in coating of the optical-fibers. Polyethylene glycol (PEG) from BDH Ltd., Poole, England is a condensation polymer of ethylene glycol with the general formula $H(OCH_2CH_2)_nOH$. The properties of PEG vary with molecular weight. It has a wide variety of applications in industry. It is used in plasticizers, softeners, mold lubricants, bases for cosmetics and pharmaceuticals, and paper coating mixtures. Two samples of PEG with average molecular weights of 3,000 (PEG3) and 20,000 (PEG20) were examined in this study. Polyacrylamide (PAA) from BDH Ltd. with molecular weight of 5,000,000 was one of the test solutions. PAA is a water soluble white powder, usually used as thickening agent, suspending agent, and additive to adhesives. Three PAA solutions were tested with the concentrations 0.25% (PAA25), 0.5% (PAA50), and 1% (PAA100). Carboxymethyl cellulose (CMC) of sodium salt (medium viscosity) from Sigma Chemical Co. (St. Louis) was also used in this study. Carboxymethyl cellulose has been used in detergents, soaps, food products (where it acts as water binder, thickener, or suspending agent), coating mixtures for paper and paper board, drilling mud, emulsion paints, pharmaceuticals, and cosmetics. The tests included four CMC solutions with the concentrations 0.5, 1, 2.5, and 5% (CMC50, CMC100, CMC250, CMC500). Surface tension coefficients of the test liquids were measured with the Fisher Surface Tensiomat which is based on the platinum-iridium ring principle of du Nouy. Densities were measured with pycnometers.

Rheology

The rheometer RheoStress RS100 from Haake was used in studying the rheological behavior of the test liquids. Some of its features are an extremely low inertia torque motor, an air bearing to center the drive shaft, a digital encoder processing 1 million impulses per revolution, a temperature sensor to allow compensation for coil heating at high torques, and multiprocessor computer control. The measured viscosity-shear rate relationships for the tested materials are displayed in Figures 2, 3, 4 and 5.

Glycerol solutions showed a Newtonian behavior at the viscosities 870 and 300 mPa·s for 100% and 95% concentrations, respectively (Table 2). Polyethylene glycol samples showed (Table 2) low Newtonian viscosities $\mu = 3.3$ and 16

Table 2. Physical Properties of Liquids

Liquid	Density kg/m^3	Surface Tension mN/m	Rheological Parameters* μ, mPa·s	n	κ, mPa·s^n	γ
Polyethylene Glycol (PEG3)	1,011.5	56.0	3.3	1.0		534
Polyethylene Glycol (PEG20)	1,013.3	43.7	16	1.0		50.9
Dilute Glycerol (Gly95)	1,253.8	53.6	300	1.0		1.34
Glycerol (Gly100)	1,260.9	66.8	870	1.0		0.406
Polydimethylsiloxane (PDMS1)	977.8	21.9	1,000	1.0		0.102
Polydimethylsiloxane (PDMS30)	992.4	23.4	25,000	1.0		0.0149
CMC50	999.5	64.8	5.5	1.0		312
CMC100	1,001.2	73.5	7.9	1.0		218
CMC250	1,009.7	74.6		0.86	380	3.47
CMC500	1,025.6	81.5		0.53	27,000	
Polyacrylamide (PAA25)	998.5	75.7		0.59	250	38.3
Polyacrylamide (PAA50)	1,000.6	75.2		0.65	600	7.85
Polyacrylamide (PAA100)	1,001.1	76.1		0.45	2,200	5.59

*$\tau = k\dot{\gamma}^n$.

mPa·s for the different molecular weights 3,000 and 20,000 respectively. Polydimethylsiloxane samples revealed mixed behavior. The lower viscosity PDMS1 showed (Table 2) a consistent Newtonian behavior ($\mu = 1{,}000$ mPa·s). The higher viscosity sample PDMS30 was Newtonian for shear rates up to 100 s^{-1} (Figure 4), and showed strong non-Newtonian shear thinning from 100 to 700 s^{-1}. Carboxymethyl cellulose solutions were Newtonian in the lower concentrations of 0.5 and 1% (Table 2), and shear thinning in the higher concentrations 2.5 and 5% (Figures 2 and 4). All polyacrylamide solutions showed strong shear thinning non-Newtonian behavior (Figure 5). The 5% CMC and PAA solutions exhibited viscoelastic features. Table 2 lists the densities, surface tension coefficients, and the rheological parameters k and n according to the power-law formula.

Viscoelastic behavior of CMC and PAA

A more thorough characterization of the liquids that exhibited viscoelastic behavior is needed. Such behavior can be studied either by a steady-state shear test, or by the measurement of the dynamic moduli in a dynamic oscillatory shear experiment. Among the liquids tested in this study, all polyacrylamide solutions and the 5% CMC solution exhibited viscoelastic behavior.

The polyacrylamide solutions were subjected to the dynamic oscillatory experiment using the cone and plate geometry, in the frequency range 0–10 rad/s. The storage modulus (G') and loss modulus (G'') for 0.5 and 1.0% PAA in the linear viscoelastic range are plotted in Figures 6 and 7. These figures reveal that the storage modulus is higher than the loss

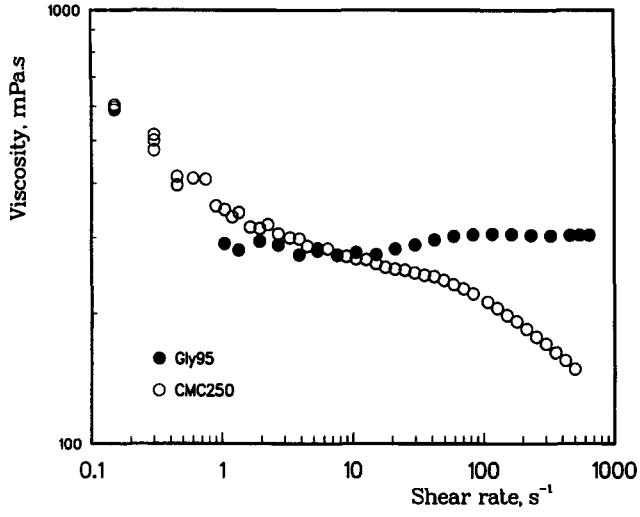

Figure 2. Viscosity of 2.5% CMC solution.

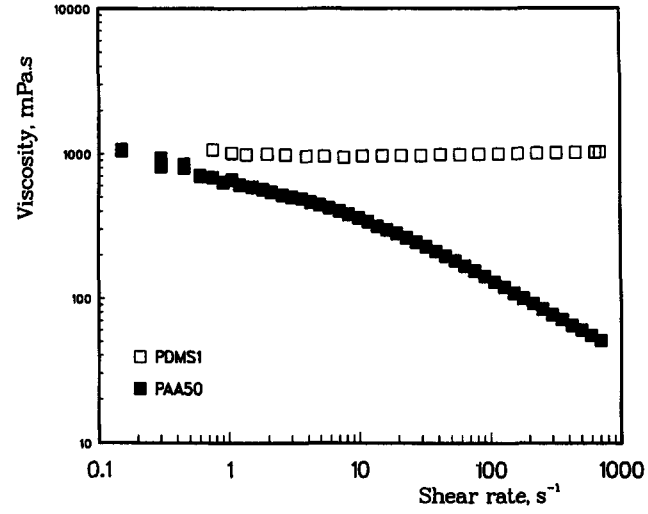

Figure 3. Viscosity of PAA50 solution.

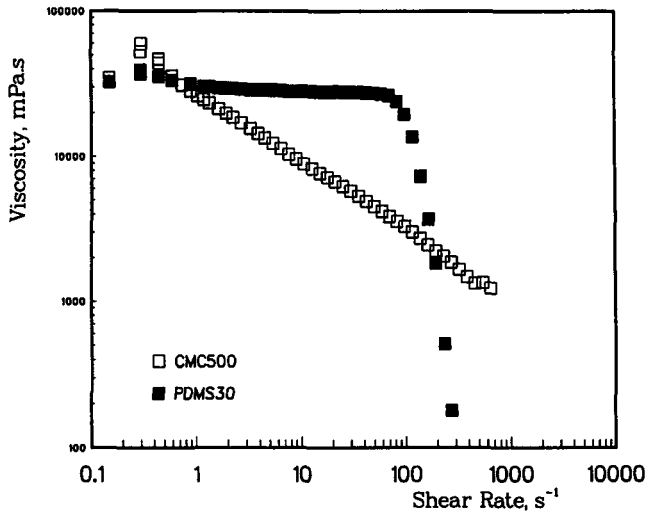

Figure 4. Viscosity of 5% CMC solution.

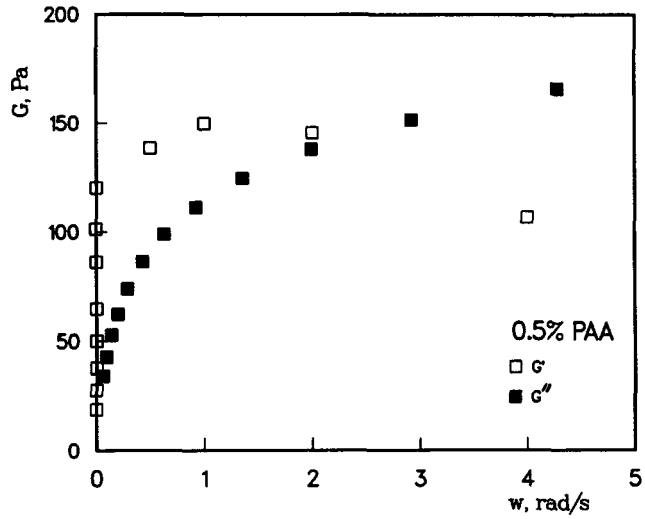

Figure 6. Storage and loss moduli, 0.5% PAA.

modulus over an initial range of frequency. This indicates that the elastic behavior is more predominant at lower frequencies. At higher frequencies, the PAA solutions show viscous behavior up to 10 rad/s. In addition, Figures 6–7 show that the frequency range responsible for elastic behavior increases with PAA concentration.

The viscoelastic behavior of 5% CMC solution was studied by testing for its response to a constant stress over a period of time. In this creep and recovery test, a preliminary experiment is run to determine the range of linear viscoelasticity. High values of applied stress usually cause a nonlinear viscoelastic response that is highly dependent on test conditions and system parameters. The linear range of viscoelasticity for 5% CMC solution was determined between 0.05 and 0.1 Pa constant stress. A stress value of 1 Pa showed a definite nonlinear viscoelasticity. Figure 8 shows the creep and recovery test for 5% CMC solution for different values of constant applied stress. The viscoelastic response is shown in terms of the compliance J, Pa^{-1} which is a material constant. Each of the constant stresses was kept for 300 s and then instantaneously removed. The 5% CMC solution shows an elastic recovery in addition to its viscous response. The response of the compliance J to the instantaneous removal of the applied stress can be seen in three steps. The initial response is a step reduction as a pure elasticity. This is followed by an exponential decrease of compliance related to a viscoelastic response. The compliance then approaches a constant limit corresponding to the nonrecovered deformation of the viscous flow.

Geometrical measurements

Experimental data, the contact angle, interfacial diameters and depths were measured by an image analysis system. A high performance color video camera CCD from Cohu, a Panasonic video cassette recorder AG-1970, and a Panasonic color monitor ST-900Y were used to record these geometrical parameters. Measurements and analysis of data were made by a system consisting of the Panasonic video cassette player AG-1970, Electrohome color monitor, 486 Everdata microcomputer, Mocha image analysis software, and TrueVision Targa plus board. This board was mounted inside the

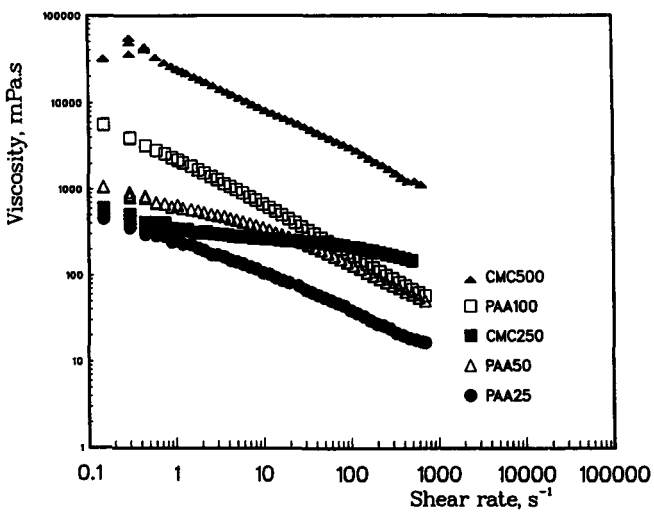

Figure 5. Viscosity of non-Newtonian liquids.

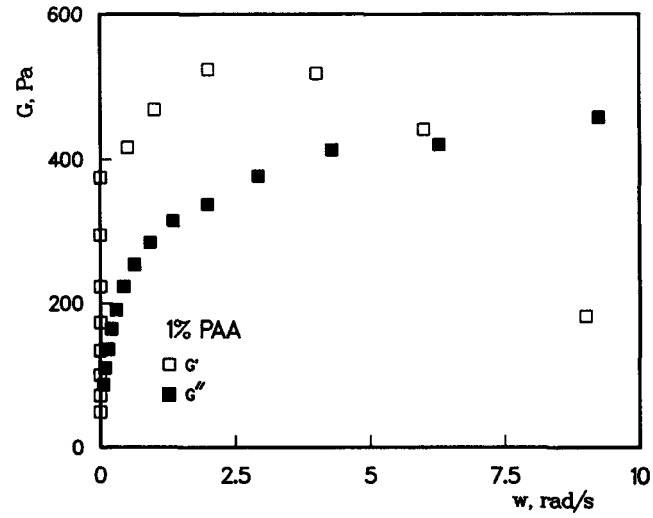

Figure 7. Storage and loss moduli, 1.0% PAA.

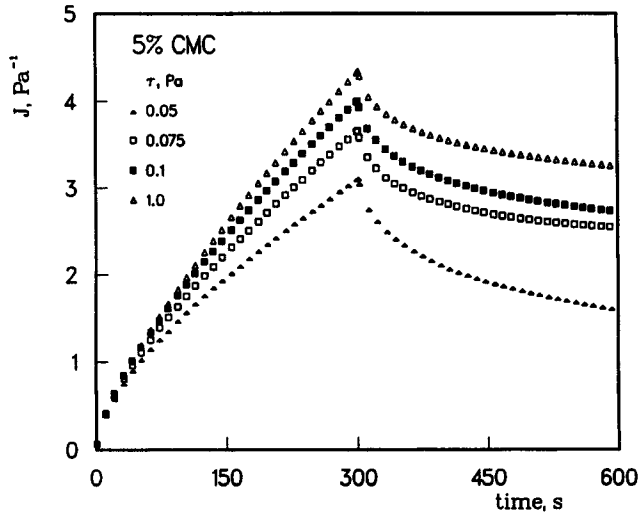

Figure 8. Compliance of CMC500.

computer to capture the video image from the monitor and to display it onto the computer screen. Each image was analyzed five times and the average values of the measured parameters were recorded.

Dimensional Analysis

The physical properties of liquids that influence the problem of surface wetting are the density ρ (kg/m^3), viscosity μ (mPa·s), and surface tension σ (kg/s^2). These properties along with gravity can be grouped in a dimensionless numbers such as those expressed in Eq. 1 (Esmail and Hummel, 1975)

$$\gamma = \sigma(\rho/\mu^4 g)^{1/3} \tag{1}$$

where g is the acceleration of gravity (m/s^2). This physical properties number primarily measures the relative contributions of viscous and surface tension forces created by the liquid. It can be used as a similarity parameter, grouping liquids of similar behavior in wetting phenomena. The dimensionless group γ is more suitable for the description of liquids in the entire wide range of viscosities. (γ is the physical properties number, $\sigma(\rho/\mu^4 g)^{1/3}$, Newtonian; $\sigma(\rho/gk^4)^{1/3}\ (V/L)^{4(1-n)/3}$, non-Newtonian.) Its values for water $\gamma \cong 3{,}000$ and alcohol $\gamma \cong 700$ are numerically reasonable. Dimensional analysis of the problem of wetting (Esmail and Ghannam, 1990) leads to the conclusion that the dynamic contact angle and other geometrical parameters of dynamic wetting depend on the capillary number (Ca) and the physical properties number γ. The capillary number is the ratio of viscous forces to surface tension forces

$$Ca = \mu V/\sigma \tag{2}$$

In this work the parameters Ca and γ need to be introduced for non-Newtonian liquids. Assuming that the rheological relationships of non-Newtonian liquids are expressed by the power-law formula

$$\tau = k\dot{\gamma}^n \tag{3}$$

then the apparent viscosity can be given as,

$$\mu = k\dot{\gamma}^{n-1} \tag{4}$$

where k is the power-law consistency (Pa·s^n). n is the power law flow index. If we take L as the characteristics length (m) of the problem and V as its characteristic velocity (m/s), then a characteristic viscosity may be expressed as

$$\mu = k(V/L)^{n-1} \tag{5}$$

The characteristic length of the wetting problem is the capillary rise (Esmail and Ghannam, 1990)

$$L = (\sigma/\rho g)^{1/2} \tag{6}$$

The capillary number of non-Newtonian liquids is then

$$Ca = \mu V/\sigma = (kV^n L^{1-n})/\sigma \tag{7}$$

The physical properties number of non-Newtonian liquids is

$$\gamma = \sigma(\rho/\mu^4 g)^{1/3} = \sigma(\rho/gk^4)^{1/3}(V/L)^{4(1-n)/3} \tag{8}$$

According to dimensional analysis (Esmail and Ghannam, 1990) dynamic contact angles are functions of these dimensionless groups

$$\theta = f(Ca, \gamma) \tag{9}$$

where θ is the contact angle (deg).

The critical capillary number that corresponds to the critical speed of air entrainment is a function of the physical properties' number γ

$$Ca_c = f(\gamma) \tag{10}$$

where Ca_c is the critical capillary number.

Results and Discussion

The study of fiber wetting with Newtonian liquids (Ghannam and Esmail, 1993) concluded that prewetting (Ghannam and Esmail, 1992) of substrates had much more impact on the values of dynamic contact angles than their shapes or geometry. Liquid properties had some influence on these angles. This influence was insignificant in the range of higher viscosity $\mu > 500$ mPa·s, or the corresponding range of lower physical properties numbers $\gamma < 0.83$. The properties of low viscosity liquids had much less influence on values of dynamic contact angles. The interfacial depth X_d (m) is (Figure 9) the distance along the substrate surface between the three-phase contact line and the horizontal level of the free surface. The linear velocity of fiber wetting influenced the interfacial depth in the same manner that it influenced the dynamic contact angle. Air is usually entrained in a wetting process when the speed exceeds a certain critical value. The critical wetting speed of air entrainment was a strong function of the degree of wetness of a surface before its wetting.

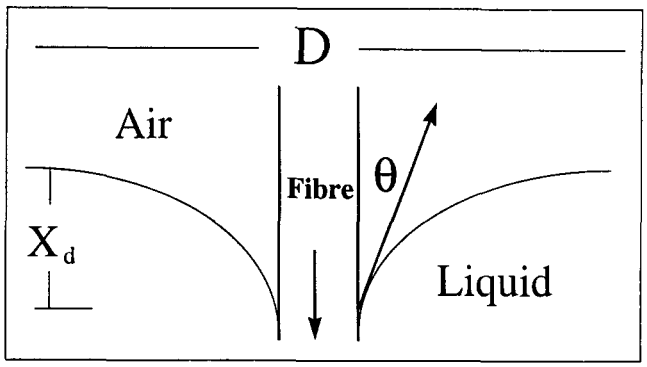

Figure 9. Definition of parameters.

For absolutely dry surfaces, the critical speed was not influenced by the geometry (plane or cylindrical) of the surface. Although there were no significant changes in the critical speed with the substrate entry angle, a slight increase was consistently present for all tested liquids when the fiber entered the liquid surface vertically. A consistent decline in the critical speed of air entrainment was recorded for all tested liquids when the fiber diameter was increased. In this work we expand the study to non-Newtonian liquids.

Dynamic contact angles

Dynamic contact angles of fiber wetting were measured for the test liquids listed in Table 2. The bottom line of our discussion at this point is that *dynamic contact angles seem to be strong functions of the apparent viscosity at the particular wetting speed regardless of whether the liquid is Newtonian or non-Newtonian.* In making this point we are assisted by the rheological curves of the test liquids that show the apparent viscosity as a function of shear rate. So we can compare viscosities at particular shear rates. First, we show (Figure 10) the clear dependence of contact angles of Newtonian test liquids on viscosities. The least viscous liquid PEG3 (Figure 10) generated the smallest contact angles over the range of velocities $0 < V < 60$ cm/s. The effect of Newtonian viscosity on angles was

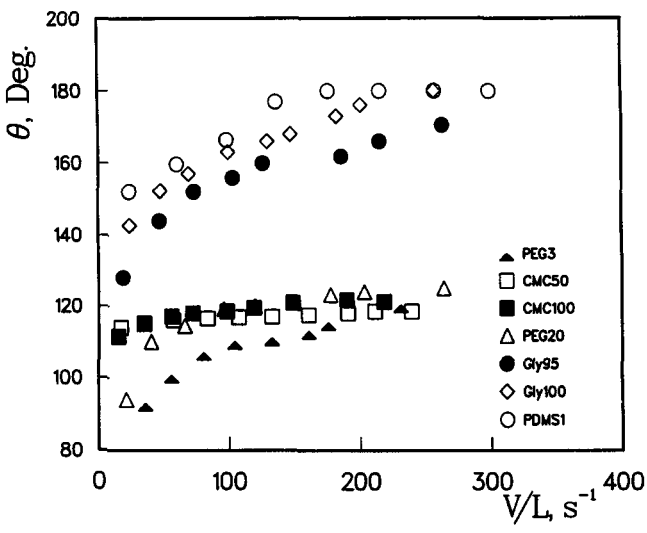

Figure 10. Contact angles, Newtonian liquids.

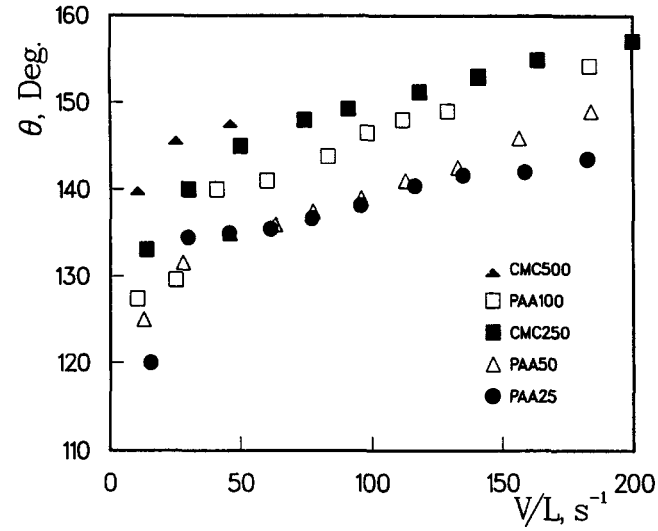

Figure 11. Contact angles of non-Newtonian liquids.

nonlinear with respect to viscosity. The solutions CMC50, CMC100, and PEG20 have reasonably close viscosities. Their contact angles clustered around the value 120° for most of the velocity range. Glycerol and PDMS1 solutions have much higher viscosity. Their angles (Figure 10) were of much higher values. Then we show three comparisons (Figures 2–4 and 12–14) between the contact angles of one Newtonian liquid and a non-Newtonian liquid with a comparable apparent viscosity at very low shear rates, and how the angles change with shear thinning of the non-Newtonian liquid. Finally, we show a comparison (Figures 5 and 11) between the contact angles of all our non-Newtonian test liquids, related to their rheological behavior, that shows the dominance of their apparent viscosities.

Dynamic contact angles were measured for a number of Newtonian liquids (Table 2) within the range of physical properties number $0.1 < \gamma < 535$. They showed a clear dependence (Figure 10) on liquid physical properties with particular dominance of viscosity. For more viscous liquids such

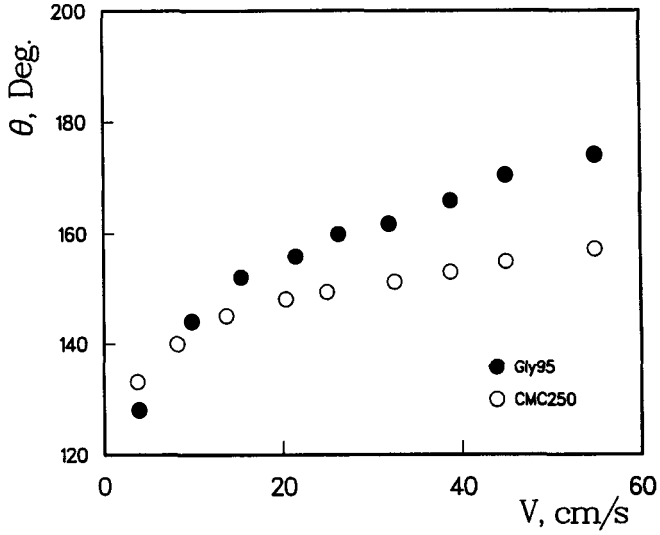

Figure 12. Contact angles, 2.5% CMC solution.

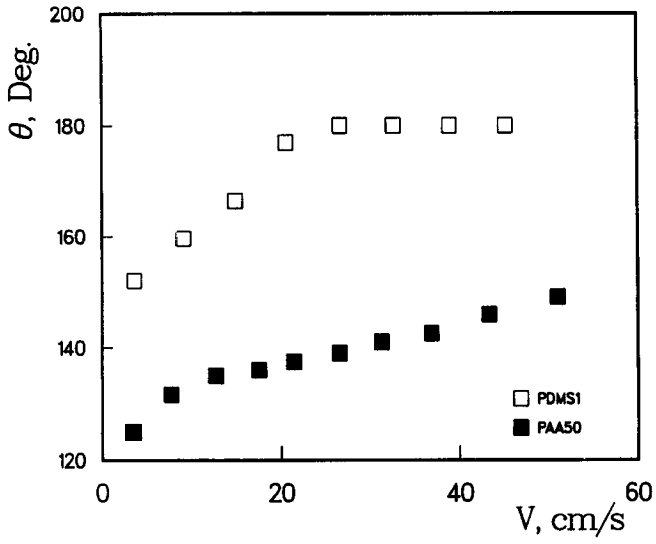

Figure 13. Contact angles, PAA50 solution.

as PDMS1 ($\mu = 1{,}000$ mPa·s) and pure glycerol ($\mu = 870$ mPa·s), contact angles rise rapidly with fiber speeds of less than 10 cm/s. Low viscosity liquids (PEG3, PEG20, CMC50 and CMC100) have much lower contact angles at speeds as high as 40–60 cm/s.

Contact angles of fiber wetting were measured with a number of non-Newtonian, primarily shear-thinning liquids (Table 2) with flow indices in the range $0.45 < n < 0.86$. Consistencies varied, but were as high as $k = 27{,}000$ mPa·s^n in the case of CMC500 solution, and as low as $k = 250$ mPa·s^n for PAA25 solution. Figure 2 shows the viscosity of 95% glycerol and 2.5% CMC solutions related to shear rate. The 2.5% CMC solution starts with an apparent viscosity of about 600 mPa·s at very low shear rates, and exhibits a mild shear-thinning non-Newtonian behavior with a flow index $n = 0.86$. The 95% glycerol solution is a Newtonian liquid with a constant viscosity of 300 mPa·s. Contact angles for the two solutions (Figure 12) were measured in the range of $0.1 < Ca < 4$ or $3 < V < 58$ cm/s. At lower wetting speeds $V < 10$ cm/s and

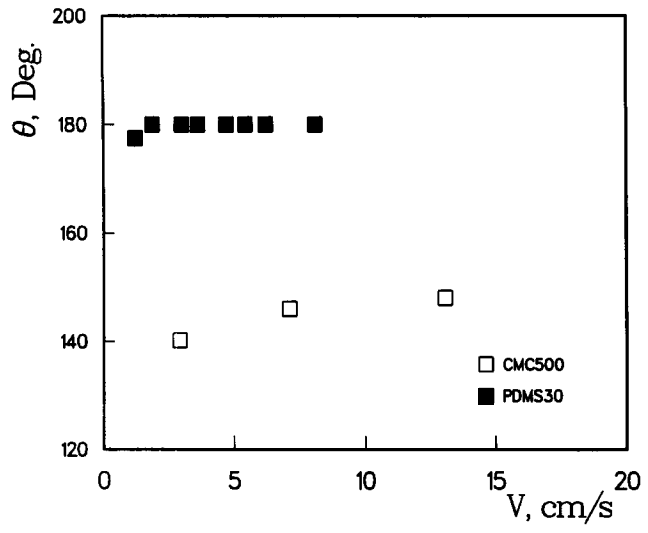

Figure 14. Contact angles, 5% CMC solution.

capillary numbers $Ca < 1$, angles measured with the 2.5% CMC solution were higher than those measured with the 95% glycerol solution. These speeds correspond to the higher values of apparent viscosity for the 2.5% CMC solution. However, when the apparent viscosity of the 2.5% CMC solution declined with shear rate (Figure 2), the dynamic contact angles (Figure 12) were lower than those measured with 95% glycerol solution at the same wetting speeds. This is an indication that *contact angles are strong functions of the apparent viscosity at the particular wetting speed regardless of whether the liquid is Newtonian or non-Newtonian.*

The viscosities of polydimethylsiloxane (PDMS1) 1,000 and 0.5% polyacrylamide PAA50 solution are shown in Figure 3. PDMS1 rheological curve shows a constant viscosity $\mu = 1{,}000$ mPa·s. The viscosity of PAA50 at very low shear rates is approximately equal to PDMS1 viscosity. However, PAA50 exhibits shear-thinning pseudoplastic behavior with a flow index $n = 0.65$. The contact angles measured for PAA50 (Figure 13) over a range of velocity $3 < V < 57$ cm/s are well below those measured with PDMS1. While PDMS1 maintains its constant viscosity of $\mu = 1{,}000$ mPa·s, the viscosity of PAA50 drops steadily to about 50 mPa·s over the corresponding range of shear rates, as shown in Figure 3. It must be noted that our apparatus could not operate at steady speeds less than 2 cm/s. This meant that we could not capture the rise in contact angles at $V < 2$ cm.

Figures 4 and 14 bring another comparison in support of the dominance of the instant apparent viscosity over the values of contact angles. The comparison here is made for liquids with much higher values of apparent viscosity. The viscosity of PDMS30 is constant at 25,000 mPa·s over a wide range of shear rates $\dot{\gamma} < 100$ s^{-1}, and then experiences a dramatic breakdown in consistency to about 200 mPa·s at a shear rate of 300 s^{-1}. The shear-thinning behavior of 5% CMC solution is described by a consistency $k = 27{,}000$ mPa·s^n and a flow index $n = 0.53$ (Table 2). Dynamic contact angles of fiber wetting were measured with 5% CMC solution for speeds less than 15 cm/s, and with PDMS30 for speeds less than 10 cm/s. In the range $2 < V < 10$ cm/s, PDMS30 is definitely Newtonian (Figure 4). Contact angles for the extremely viscous PDMS30 (Figure 14) increase rapidly to the limit 180° at a wetting speed of about 2 cm/s. Air was entrained in all runs with PDMS30. In order to capture the rise in the contact angle of fiber wetting with such an extremely viscous liquid, one should use an apparatus where steady wetting speeds of millimeters per second can be achieved. At the high concentration of 5%, CMC forms gel structure which easily breaks down under the effect of fiber line shear. The contact angles of fiber wetting with 5% CMC solution (Figure 14) were much lower than those for PDMS30, although both liquids had comparable viscosities at very low shear rates. The breakdown in the CMC structure is responsible for lowering the dynamic contact angle. Measurements with the 5% CMC solution above $V = 20$ cm/s showed strong instability in the form of a widely oscillating contact angle that could not be recorded. This may be an elastic instability related to the viscoelasticity of CMC500 (Figure 8).

The comparison between all non-Newtonian test liquids is shown in Figures 5 and 11. First, we would like to focus attention on the three polyacrylamide solutions. In rheological tests, polyacrylamide 0.25, 0.5 and 1% solutions reveal a

shear-thinning behavior with different consistencies and flow indices as shown in Figure 5 and Table 2. In dynamic oscillatory tests, PAA solutions showed viscoelastic behavior (Figures 6 and 7). Their apparent viscosities at very low shear rates are about 450, 1,000 and 5,500 mPa·s, respectively. According to Figure 5, the increase in shear rate tends to move the PAA50 viscosity away from PAA25 viscosity, and closer to that of PAA100, although all viscosities are declining. Angles measured with PAA50 (Figure 11) are very close to those measured for PAA25 up to a wetting speed of about 37 cm/s. However, for higher speeds they diverge moving closer to those measured for PAA100. This behavior is consistent with the change in their apparent viscosities. The contact angles measured for 2.5% CMC solution (Figure 11) also show the dominance of apparent viscosity (Figure 5). This solution has the highest flow index $n = 0.86$ among all our shear-thinning test liquids (Table 2). In the range of shear rates $100 < \dot{\gamma} < 1{,}000$, its apparent viscosity in Figure 5 is higher than that of other liquids except the 5% CMC solution. Its contact angles are definitely higher in Figure 11 than all angles except those of the 5% CMC solution. The apparent viscosities at particular shear rates exert dominant influence on contact angles of non-Newtonian liquids.

It appears that fiber diameter has some influence on the values of dynamic contact angles. Figure 15 shows contact angles of fiber wetting with a 95% glycerol solution for three different fiber diameters. *Higher values of contact angles correspond to wetting of fiber with smaller diameter.* A decrease in fiber diameter increases surface tension force. However, in our experiments no such effect was observed (Figure 16) for fiber wetting with PDMS1, a liquid with much higher viscosity ($\mu = 1{,}000$ mPa·s) than the 95% glycerol solution ($\mu = 300$ mPa·s). The influence of fiber diameter may be limited to lower viscosity liquids.

The most convenient form of making our measurements of contact angles available to other users is regression analysis of the experimental data. Dimensional analysis showed that the dynamic contact angle is a function of the two dimensionless groups, the capillary number and the physical properties number

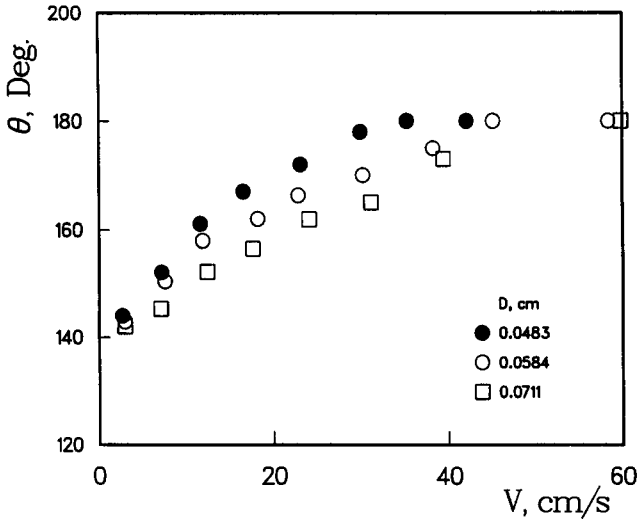

Figure 15. Contact angles for different fiber diameters, Gly95.

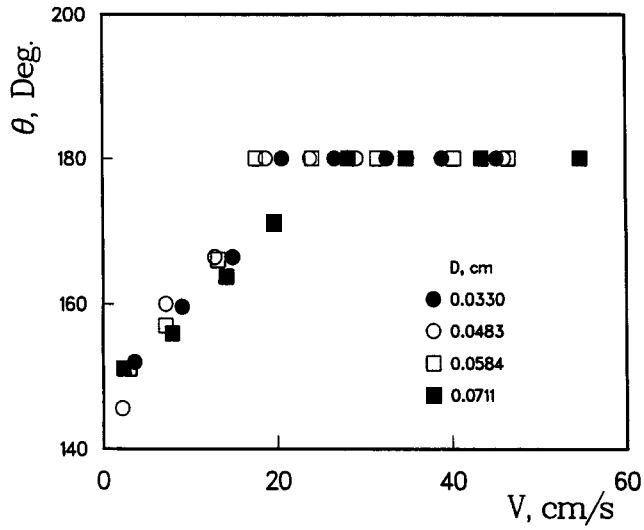

Figure 16. Contact angles for different diameters, PDMS1.

$$\theta = f(Ca, \gamma) \tag{9}$$

Therefore for each particular liquid, characterized by a specific value of the parameter γ the dynamic contact angle is a function of the capillary number and may be represented by regression analysis as

$$\theta = a\,Ca^{b} \tag{11}$$

where a is the proportionality regression coefficient, and b is the power regression coefficient. Regression analysis for our experimental measurements of the dynamic contact angles was carried out. Table 3 shows values of a and b and the regression coefficient r for all the test liquids.

As we mentioned earlier, at a critical value of the wetting speed, small visible air bubbles are entrained into the liquid by the fiber line. The capillary number and the physical properties number are the important parameter groups in the phenomenon of air entrainment. Figure 17 shows the dimensionless correlation between the critical capillary number corresponding to the onset of air entrainment and the physical properties number for liquids tested in this work. *Critical capillary numbers of shear thinning liquids are generally higher than those of Newtonian liquids.*

Table 3. Results of Regression Analysis

Solution	γ	a	b	r
PEG3	534	179.54	0.119	0.98
PEG20	50.9	147.25	0.092	0.88
Gly95	1.34	152.43	0.113	0.99
Gly100	0.406	145.41	0.097	0.99
PDMS1	0.102	145.72	0.076	0.94
PDMS30	0.149×10^{-2}	175.98	0.005	0.80
CMC50	312	123.59	0.015	1.00
CMC100	218	131.56	0.029	0.94
CMC250	3.47	153.62	0.069	0.99
PAA25	38.3	170.09	0.102	0.88
PAA50	7.85	149.44	0.133	0.97
PAA100	5.59	162.14	0.128	0.94

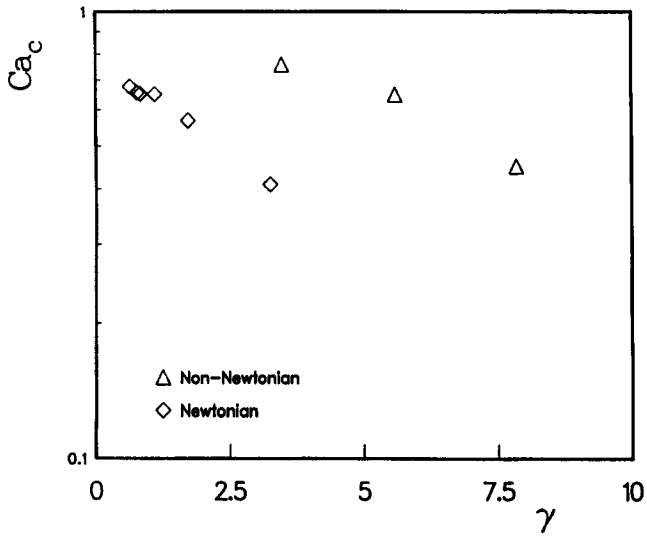

Figure 17. Critical conditions of air entrainment.

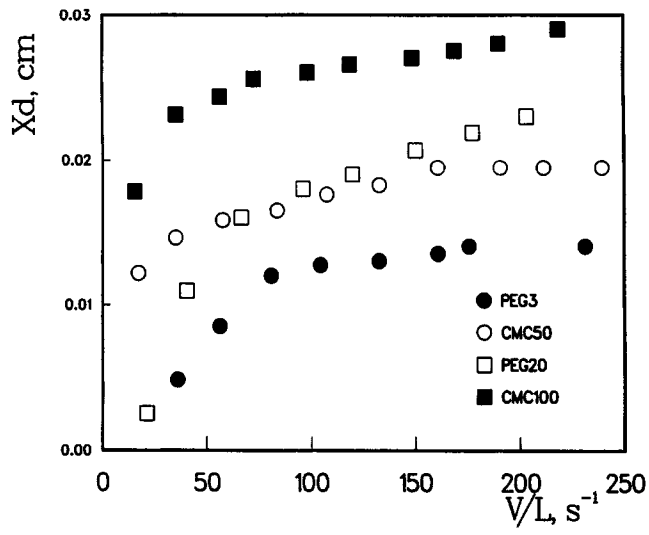

Figure 19. Interfacial depth, smallest scale.

Interfacial diameters and depths

The depression created in the liquid surface by the steadily plunging fiber is characterized by a number of parameters including the dynamic contact angle. Two such parameters are the interfacial depth and diameter. The interfacial depth is the distance along the the fiber axis between the contact line and the horizontal level of the liquid volume. The interfacial diameter is the diameter of the circle bordering the depression. For the sake of completeness of our investigation we measured both parameters. *The depressions created in the surface of different test liquids can be classified into three different scales.* The smallest scale of depression belongs to four Newtonian liquids, PEG3, PEG20, CMC50, and CMC100 solutions (Figures 18 and 19). The orders of magnitude of the interfacial diameter in this case was 1–3 mm, and that of the interfacial depth was 0.1–0.3 mm. Viscosities of this group of test liquids are in the lower range $\mu < 16$ mPa·s. The second scale of depressions (Figures 20 and 21) was created by pure glycerol, 95% glycerol solution, PDMS1, 2.5 % CMC solution, 0.25%, and 1% PAA solutions. The orders of magnitude for this scale were 0.5–2 cm for the interfacial diameter, and 0.1–0.5 cm for the interfacial depth. Viscosities of these liquids in the range of measured wetting speeds are $100 < \mu <$ 8,000 mPa·s. The liquids PDMS30 and 5% CMC solution experienced the largest depressions (Figures 22 and 23) with interfacial diameters around 2–4 cm, and interfacial depths close to 0.5–1.25 cm. Their viscosities are $4{,}000 < \mu < 30{,}000$ mPa·s, but primarily above 10,000 mPa·s. In general, *experiments showed that the interfacial depth and diameter are strong functions of the apparent viscosity at the particular wetting speed regardless of whether the liquid is Newtonian or non-Newtonian.* Comparison of interfacial depths and diameters using fibers with different diameters showed no evidence of influence by the fiber diameter.

Conclusions

Dynamic contact angles seem to be strong functions of the apparent viscosity at the particular wetting speed regardless

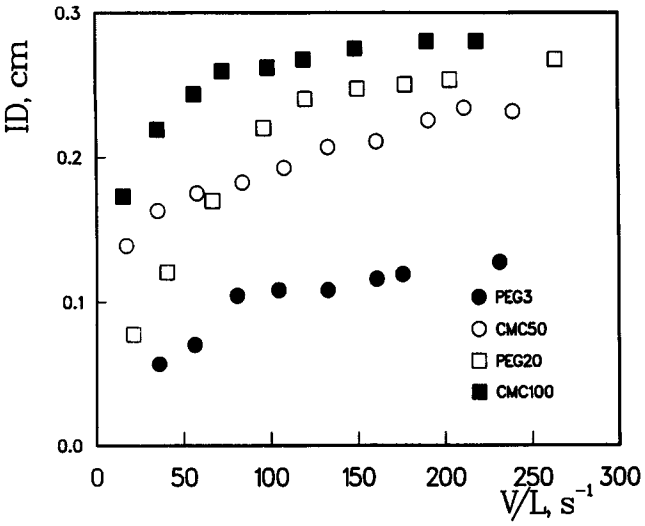

Figure 18. Interfacial diameter (ID, m), smallest scale.

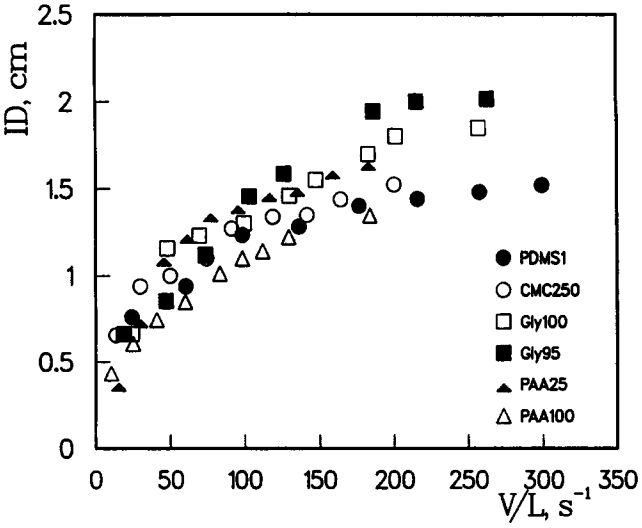

Figure 20. Interfacial diameter, intermediate scale.

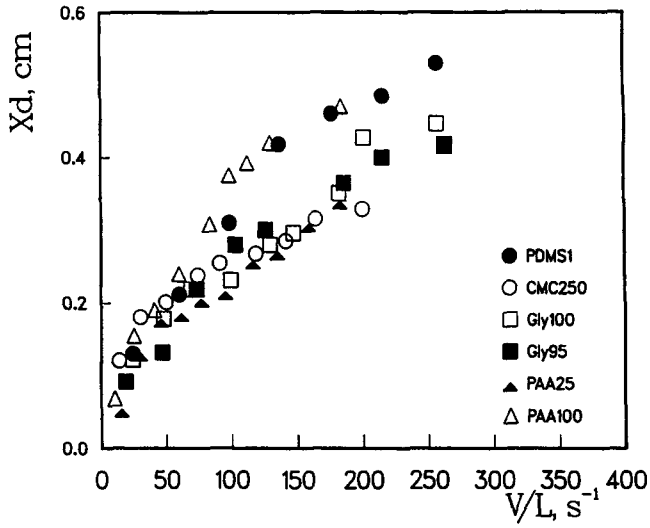

Figure 21. Interfacial depth, intermediate scale.

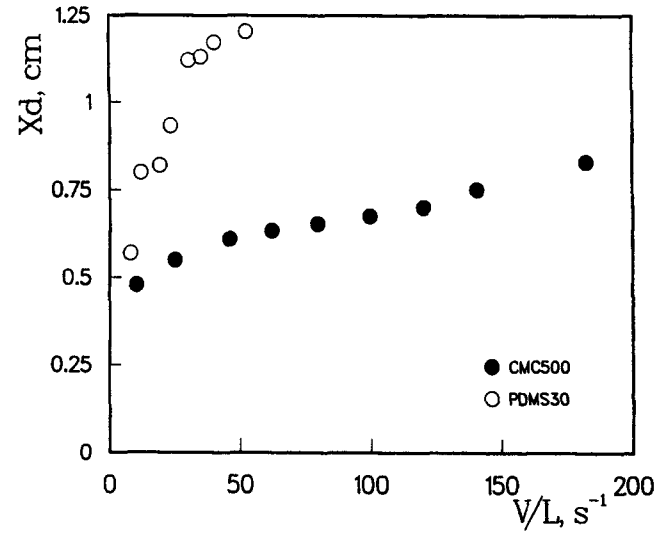

Figure 23. Interfacial depth, large scale.

of whether the liquid is Newtonian or non-Newtonian. Contact angles of Newtonian liquids showed a clear dependence on liquid physical properties with particular dominance of viscosity. Comparisons between the contact angles of Newtonian and a non-Newtonian liquids with comparable apparent viscosities at very low shear rates show how the angles change with the shear thinning of the non-Newtonian liquid. Comparison between all our non-Newtonian test liquids, related to their rheological behavior, shows the dominant influence of their apparent viscosities on contact angles. Higher values of contact angles correspond to wetting of fiber with smaller diameter for less viscous liquids. Critical capillary numbers of air entrainment for shear thinning liquids are generally higher than those for Newtonian liquids. The depressions created in the surface of different test liquids can be classified into three different scales, corresponding to three scales of liquid viscosities.

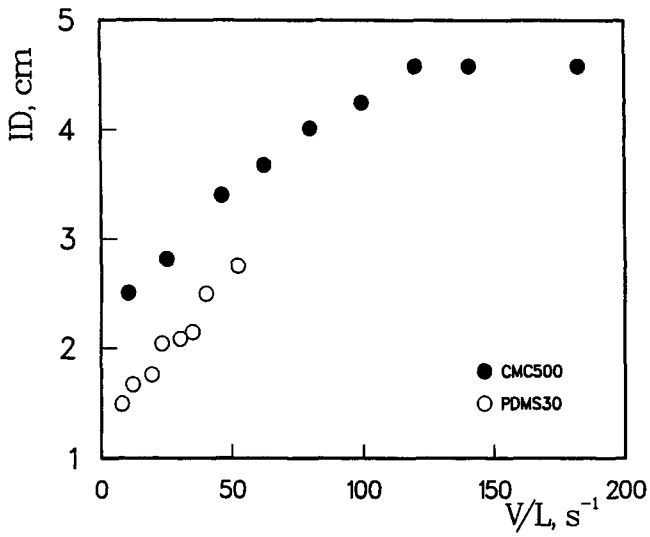

Figure 22. Interfacial diameter, large scale.

Literature Cited

Blake, T. D., "Wetting Kinetics—How Do Wetting Lines Move?," AIChE Meeting, New Orleans (Mar. 7–10, 1988).

Burley, R., "Mechanisms and Mechanics of Air Entrainment in Coating Processes," *Ind. Coating Res.*, **2** (1992).

Esmail, M. N., and R. L. Hummel, "Nonlinear Theory of Free Coating Onto a Vertical Surface," *AIChE J.*, **21**, 958 (1975).

Esmail, M. N., and M. T. Ghannam, "Air Entrainment and Dynamic Contact Angles in Hydrodynamics of Liquid Coating," *Can. J. Chem. Eng.*, **68**, 197 (1990).

Ghannam, M. T., "Air Entrainment and Dynamic Contact Angles in Hydrodynamics of Liquid Coating," PhD Thesis, University of Saskatchewan (1991).

Ghannam, M. T., and M. N. Esmail, "The Effect of Pre-Wetting on Dynamic Contact Angles," *Can. J. Chem. Eng.*, **70**, 408 (1992).

Ghannam, M. T., and M. N. Esmail, "Experimental Study of the Wetting of Fiber," *AIChE J.*, **39**, 361 (1993).

Gutoff, E. B., and C. E. Kendrick, "Dynamic Contact Angles," *AIChE J.*, **28**, 459 (1982).

Joos, P., M. Bracke, and V. Remoortere, "The Dynamic of Wetting," AIChE Meeting, Orlando (1990).

Miyamoto, K., "On the Mechanism of Air Entrainment," *Ind. Coating Res.*, **1** (1991).

Perry, R. T., "Fluid Mechanics of Entrainment Through Liquid-Liquid and Liquid-Solid Junction," PhD Thesis, Univ. of Minnesota (1967).

Manuscript received Aug. 15, 1996, and revision received Feb. 18, 1997.